OPEN

Demonstration and Mitigation of Aerosol and Particle Dispersion During Mastoidectomy Relevant to the COVID-19 Era

*†Jenny X. Chen, *†Alan D. Workman, *†Divya A. Chari, *†David H. Jung, *†Elliott D. Kozin, *Daniel J. Lee, *†D. Bradley Welling, *†Benjamin S. Bleier, and *†Alicia M. Quesnel

*Department of Otolaryngology – Head and Neck Surgery, Massachusetts Eye and Ear; and †Department of Otolaryngology – Head and Neck Surgery, Harvard Medical School, Boston Massachusetts

Background: COVID-19 has become a global pandemic with a dramatic impact on healthcare systems. Concern for viral transmission necessitates the investigation of otologic procedures that use high-speed drilling instruments, including mastoidectomy, which we hypothesized to be an aerosol-generating procedure.

Methods: Mastoidectomy with a high-speed drill was simulated using fresh-frozen cadaveric heads with fluorescein solution injected into the mastoid air cells. Specimens were drilled for 1-minute durations in test conditions with and without a microscope. A barrier drape was fashioned from a commercially available drape (the OtoTent). Dispersed particulate matter was quantified in segments of an octagonal test grid measuring 60 cm in radius.

Results: Drilling without a microscope dispersed fluorescent particles 360 degrees, with the areas of highest density in quadrants near the surgeon and close to the surgical site. Using a microscope or varying irrigation rates did not significantly reduce particle density or percent surface area with particulate. Using the OtoTent significantly reduced particle density and percent surface area with particulate across the segments of the test grid beyond 30 cm (which marked the boundary of the OtoTent) compared with the microscope only and no microscope test conditions (Kruskall–Wallis test, $p = 0.0066$).

Conclusions: Mastoidectomy with a high-speed drill is an aerosol-generating procedure, a designation that connotes the potential high risk of viral transmission and need for higher levels of personal protective equipment. A simple barrier drape significantly reduced particulate dispersion in this study and could be an effective mitigation strategy in addition to appropriate personal protective equipment.

Key Words: Aerosol—Aerosolgenerating procedures—Barrier drape—Coronavirus COVID-19—Mastoidectomy—Otologic surgery—OtoTent—Personal protective equipment—SARS CoV-2.

Otol Neurotol **41:**1230–1239, 2020.

The novel severe acute respiratory syndrome coronavirus 2 (SARS-CoV-19) causing the disease COVID-19 emerged in Wuhan, China, in November 2019 and has since spread rapidly across the globe, causing the World Health Organization to declare the outbreak a pandemic on March 11, 2020 (1). Hospital systems in affected regions continue to face a surge of patients and struggle in the setting of shortages of testing materials, rapid testing strategies, ventilators, and personal protective equipment (PPE) for hospital staff (2).

Early reports of healthcare worker infections in China and Italy suggested high rates of infection among otolaryngologists (3–5). COVID-19 is believed to be spread through not only droplets but also aerosols during a variety of aerosol-generating procedures that otolaryngologists routinely perform. These range from office-based procedures like flexible nasopharyngoscopy and peritonsillar abscess drainage (6) to operative procedures such as intubation/extubation (7,8), tracheotomy (9), maxillofacial trauma surgery (10), as well as endoscopic sinus and skull base surgery (4,11).

Otologic surgery including mastoidectomy has not been explicitly described as an aerosol-generating procedure, which is an important distinction that connotes the potential increased risk of viral transmission and the need for PPE designated for aerosol-generating procedure. Existing studies suggest that the use of high powered drills is associated with the generation of aerosols and small particles with the potential to transmit

Address correspondence and reprint requests to Alicia M. Quesnel, M.D., 243 Charles Street, Boston, MA 02114; E-mail: alicia_quesnel@meei.harvard.edu

J.X.C. and A.D.W. contributed equally to this work.

The authors disclose no conflicts of interest.

Supplemental digital content is available in the text.

DOI: 10.1097/MAO.0000000000002765

infectious diseases (11–13). As the airway is continuous with the middle ear and mastoid, there is potential for viral transmission of COVID-19 from otologic procedures (14). An improved understanding of procedures that generate aerosols and small droplets is necessary to balance the need to protect health care workers with the desire to conserve limited stocks of PPE (6). In this study, we sought to demonstrate that mastoidectomy is an aerosol-generating procedure and explored a simple barrier strategy to mitigate the risk for viral transmission.

METHODS

Preparation of Specimen and Supplies

Three ears from two fresh-frozen cadaveric head specimens were prepared. Standard C-shaped postauricular skin incisions were made and anteriorly based periosteal flaps were elevated. Fluorescein solution was created with 50 mL of sterile water mixed with 1 mg of FUL-GLO Fluorescein Sodium (Akorn, Inc., Lake Forest, IL). The mastoid cortex was drilled to expose a 4 × 4 mm area of air cells and 1.5 mL of fluorescein solution was injected into this well. The Midas Rex Legend Stylus otologic drill with a compatible Xomed 6 mm round fluted bur (Medtronic, Inc., Minneapolis, MN) was used. Images and videos were captured on a dual-lens camera system with a 12MP camera with a wide-angle lens with f/1.8 aperture and 4K video recording system at 60 frames per second (Apple, Inc., Cupertino, CA). The microscope was a wall-mounted Zeiss OPMI Pico (Carl Zeiss Meditec AG, Jena, Germany) with an objective lens focal distance of 250 mm. An ultraviolet light source, UV-705, 400-Watt (Altman Lighting, Yonkers, NY) was used and all fluorescent images were taken in a darkened room. A 1,060 Steri-Drape of 130 cm × 130 cm in size with an incise film in the center of 10 cm × 12.5 cm was used (3M, Inc., St. Paul, MN) for the barrier drape.

Experimental Setup

A separate thawed cadaveric temporal bone was used for each primary condition. A single, right-handed surgeon drilled for 1 minute for each condition; the surgeon's surgical gown and mask were photographed under ultraviolet light to evaluate for fluorescent debris (Fig. 1). The cadaveric head was placed in the center of a black mat in a standard surgical position. Using the external auditory canal (EAC) as the center point, an octagonal grid with a radius of 60 cm was marked out around the specimen (Fig. 2, A and B). After each experiment, particulate matter was examined in each segment of the octagonal test grid (Fig. 2C).

The primary conditions tested were 1) open field (no microscope or barrier drape); 2) microscope without a drape; and 3) microscope with a drape. All three primary conditions were tested with 10 mL/min irrigation. Two additional conditions in an open field were tested: high irrigation (20 mL/min) and no irrigation. After drilling in each condition, photos were taken of the octagonal grid (Fig. 2) for further image processing and particle counts. The black mat was cleaned between experiments.

Barrier Drape

The 1,060 Steri-drape (Fig. 3A) was used to create a barrier drape that enclosed the microscope lens, cadaveric head specimen, and immediate surrounding 30 cm surgical field (here forward referred to as the ''OtoTent''). A hole with a 6 cm diameter was cut into the incise film (with adhesive backing) in the center of the 1,060 Steri-drape (Fig. 3B). The hole in the drape was aligned with the microscope lens so that the lens was not obstructed, and the surrounding adhesive part of the drape was secured around the outside of the lens mount (Fig. 3, A and B). The drape was placed over the cadaveric head. The excess drape was loosely rolled under and secured to the mat in four cardinal points 30 cm away from the EAC with tape: superior, inferior, posterior, and anterior (Fig. 4A). The surgeon's arms and instruments were passed under the drape, on either side of

FIG. 1. Aerosolization of fluorescent bone dust and droplets occurs during mastoidectomy. *A*, The aerosol plume created by using a high-speed otologic drill to perform a cortical mastoidectomy is visible in a darkened room under ultraviolet light. Surgeon is using a size 6 cutting bur, at 70,000 RPM, on a cadaveric specimen. See Supplemental Video 1, http://links.lww.com/MAO/B24 {Aerosolization of fluorescent droplets and bone particulate from cortical mastoidectomy is demonstrated on a cadaveric specimen under an ultraviolet light in a darkened room. The OtoTent preparation and use with the microscope is shown.}. *B*, Fluorescent debris (some indicated by green *arrowheads*) soiling a surgeon's chest, arms, and lap is shown under ultraviolet light after drilling part of a cortical mastoidectomy for 2 minutes, with size 6 cutting bur, at 70,000 RPM. *C*, Image showing fluorescent particulate matter scattered on the surgeon's face shield and hair covering (green *arrowheads*) after 2 minutes of drilling.

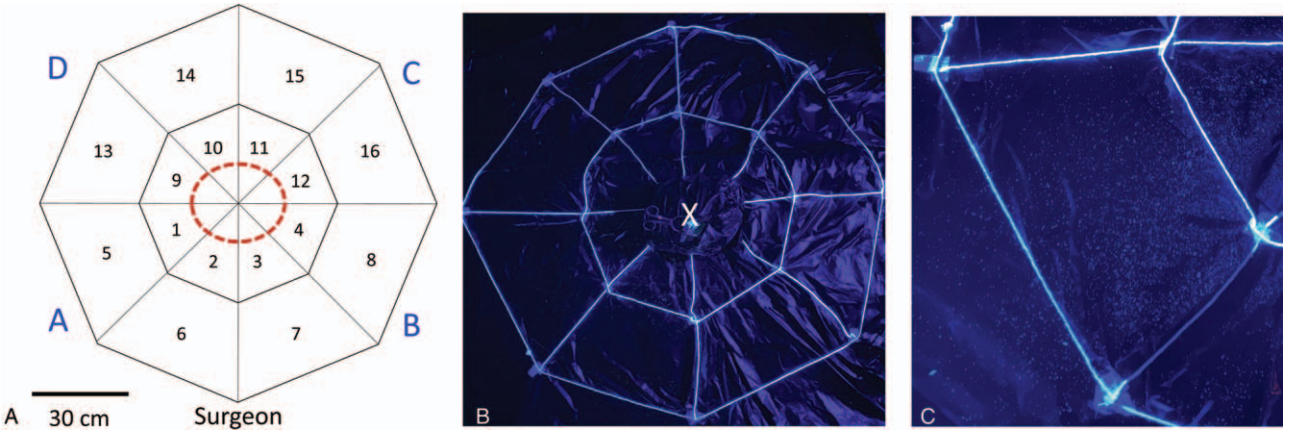

FIG. 2. Experimental setup. *A*, Octagonal grid created to define distances and locations of particulate debris from the ear canal. The inner octagon has a radius of 30 cm and the outer octagon has a radius of 60 cm. The cadaveric head specimen was placed in the center (red dotted *circle*). Segments of the grid are numbered (small black font), and quadrants are labeled (large blue font) for reference in the text. *B*, Sample aerial photo of grid under ultraviolet light with the cadaveric specimen marked by the "X". *C*, Sample close-up photo of one segment of the grid with numerous fine fluorescent particles, representing bone dust or fluorescein stained droplets.

the posterior point of tape fixation, to perform surgery (Fig. 4B). Following the experiment, the drape was lifted to reveal fluorescent tissue particles on the undersurface (Fig. 4C).

Image Processing, Quantification, and Statistical Analysis

ImageJ software (version 2.0.0-rc-69/1.52p) was used for image manipulation and particle analysis. Images were cropped to include only the segment to be analyzed in each iteration. The background was subtracted algorithmically using a rolling ball radius of 5 pixels, with separated colors and the sliding paraboloid method to remove background reflected light and heterogeneous surface reflection. Following this, color adjustment was performed to eliminate red and blue hues. The image was checked for consistency and nonparticulate edges were removed manually. The image was changed to an 8-bit image, and a binary black and white pixel threshold was applied. Particle analysis was run with a particle size 0-infinity, circularity 0.0–1.0, with particle counting and percent area calculation. GraphPad Prism version 8.0 (La Jolla, CA) was used for descriptive statistics. Nonparametric tests (Kruskall–Wallis test, Mann–Whitney *U* test, two-stage linear step up procedure of Benjamini, Krieger, Yukutieli for multiple comparisons) were used to compare particle surface density and percent surface area covered by particles in different regions of the test grid.

RESULTS

Videos and still images of drilling in an open field and drilling with a microscope demonstrated large plumes of fluorescent aerosolized materials (Fig. 1A, Supplemental Video 1, http://links.lww.com/MAO/B24 {Aerosolization of fluorescent droplets and bone particulate from cortical mastoidectomy is demonstrated on a cadaveric specimen under an ultraviolet light in a darkened room. The OtoTent preparation and use with the microscope is

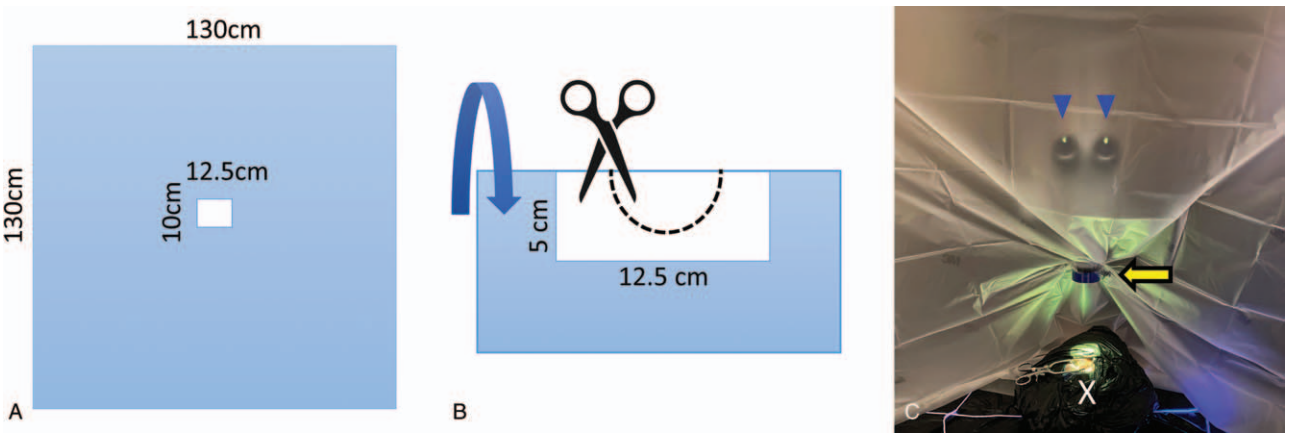

FIG. 3. Preparing the OtoTent. *A*, Sketch of an opened 1,060 3M drape. The central 10 × 12.5 cm portion of the drape is backed in adhesive. *B*, Sketch showing how a hole is cut in the adhesive portion of the drape to allow for the microscope lens. *C*, Photo of the OtoTent in position on the microscope, with the edge of the drape lifted. The microscope oculars (blue *arrowheads*), microscope lens (yellow *arrow*), and cadaveric specimen (X) are marked for orientation.

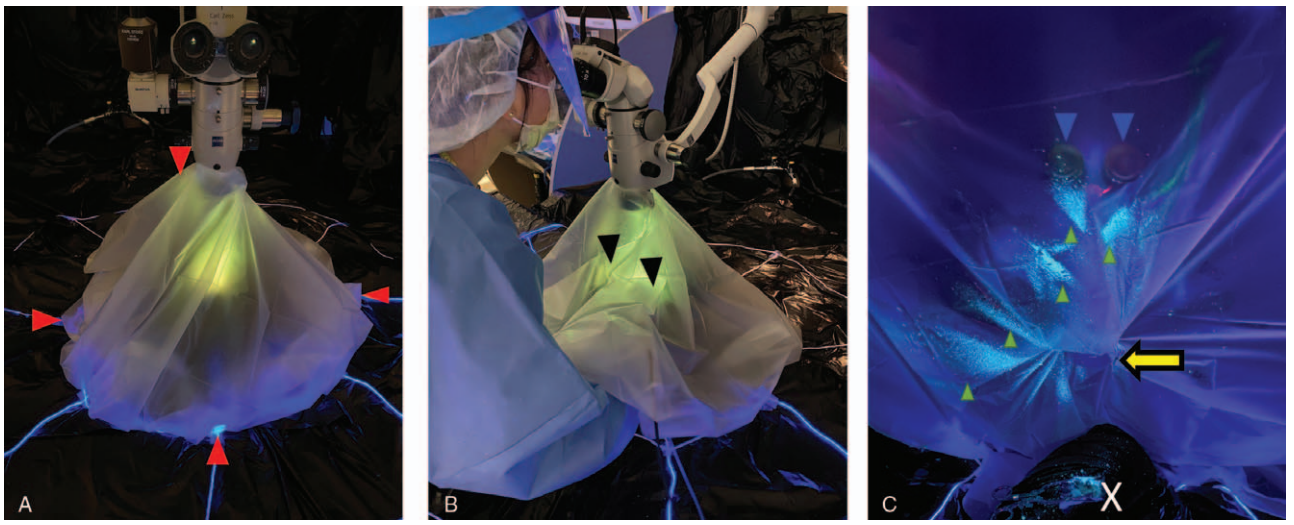

FIG. 4. Positioning and using the OtoTent. *A*, The drape was secured at cardinal points 30 cm away from the EAC of the specimen using adhesive tape: superior, inferior, posterior, and anterior (red *arrowheads*). *B*, Photo of surgeon operating under the OtoTent. Black *arrowheads* indicate the positions of the hands underneath the drape. *C*, Photo of the underside of the OtoTent after drilling for 60 seconds. The edge of the drape is lifted up to show the fluorescent particles densely adherent to the underside of the drape (green *arrowheads*). The microscope lens (yellow *arrow*) and cadaveric specimen (X) are marked for orientation. EAC indicates external auditory canal.

shown.}). Photographs of the surgeon's gown, face shield, and hair covering revealed a heavy burden of contamination within minutes of drilling (Fig. 1B, C). The patterns of aerosol and particulate dispersion among the three test conditions (open field, microscope without OtoTent, and microscope with OtoTent) over the octagonal test grid are shown in Figure 5. Particles, including bone dust and fluorescein droplets, were found in every quadrant in every experimental condition. Particulate size ranged from 100 μm to 4.6 mm, with > 99% of

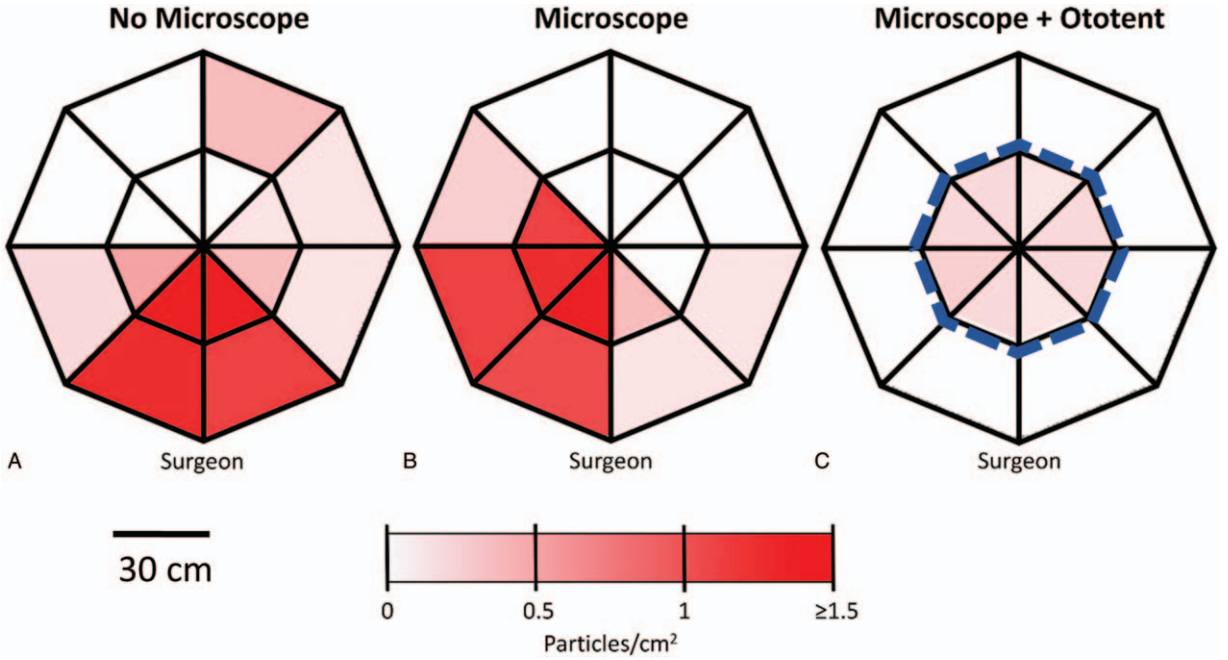

FIG. 5. Heat map of the surface density of fluorescent particles found in each grid segment after each test condition. *A*, Simulation without the microscope shows a predominance of particles in the quadrants closest to the surgeon (quadrants 1 and 2—see Fig. 2A for quadrant labeling). There is also particulate dispersion away from the surgeon, illustrating the importance of considering strategies that offer protection to nearby operating room staff. *B*, The addition of the microscope still results in particulate dispersion that is highest in quadrants 1 and 2 (adjacent to the surgeon), and also still demonstrates particulate dispersion away from the surgeon (potentially toward other operating room staff). *C*, Simulation with the OtoTent (blue dotted lines) shows decreased particulate matter in all areas, including both the inner and outer octagons. Note the OtoTent drape was fixed at four cardinal points at a radius of 30 cm, thus enclosing the inner octagon on the grid. Note that particulate surface density is close to zero in the surrounding outer octagon, outside the OtoTent barrier.

TABLE 1. *Percent surface density (PSD) and percent surface area (%SA) covered in particulate after drilling in each test condition*

	Quadrant Mean (SD)			
	A	**B**	**C**	**D**
Open field				
PSD	1.55 (1.74)	0.86 (0.79)	0.16 (0.14)	0.11 (0.08)
%SA	1.01 (0.99)	0.50 (0.44)	0.04 (0.02)	0.07 (0.05)
Microscope only				
PSD	1.35 (0.37)	0.16 (0.13)	0.03 (0.02)	0.38 (0.47)
%SA	0.95 (0.34)	0.10 (0.08)	0.01 (0.01)	0.26 (0.29)
Microscope+OtoTent				
PSD	0.16 (0.13)	0.10 (0.09)	0.11 (0.11)	0.13 (0.11)
%SA	0.11 (0.11)	0.07 (0.08)	0.07 (0.08)	0.11 (0.10)

SD indicates standard deviation.

particles between 100 μm and 1 mm in size. Owing to the image resolution, particulates smaller than 100 μm could not be evaluated.

Simulation of Mastoidectomy Without Microscope

Fluorescein droplets and bone dust dispersed to all segments of the grid in a 360-degree fashion, with particle surface density (PSD) ranging from 0.036 to 4.0 particles/cm^2 and percent surface area with particulate (%SA) ranging from 0.011 to 2.3% (Table 1). The highest PSD and %SA were found in quadrants A and B, representing quadrants closer to the surgeon (PSD $1.55 \pm$ standard deviation, SD, 1.74, %SA 1.01 ± 0.99; PSD 0.86 ± 0.79, %SA 0.50 ± 0.44 respectively; Table 1, Fig. 5A). There was less particulate matter in quadrant C than the quadrants nearer to the surgeon (PSD 0.16 ± 0.14, %SA 0.04 ± 0.02) and the least amount was found in quadrant D (PSD 0.11 ± 0.08, %SA 0.07 ± 0.05; Table 1, Fig. 5A).

Qualitative assessment of the table beyond the 60 cm radius of the octagonal grid revealed fluorescent particulate debris in both the front left and right corners of the table after drilling, at a distance of 114 cm from the EAC. Further distances could not be assessed with this experimental setup.

Simulation of Mastoidectomy With Microscope

Fluorescein droplets and bone dust were found in all areas of the experimental grid (Fig. 5B) with PSD ranging from 0.011 to 1.74 particles/cm^2 and %SA ranging from 0.004 to 1.3% (Table 1). The highest PSD and %SA were found in quadrant A (PSD 1.35 ± 0.37, %SA 0.94 ± 0.34) and the lowest were found in quadrant C (PSD 0.03 ± 0.02, %SA 0.01 ± 0.01; Table 1, Fig. 5B).

Simulation of Mastoidectomy With Microscope and OtoTent

Fluorescein droplets and bone dust were found at low levels across all areas of the experimental grid (Fig. 5C) with no areas of predominance in terms of radial direction. PSD ranged from 0.018 to 0.29 particles/cm^2 and %SA ranging from 0.008 to 0.25% (Table 1). For the microscope + OtoTent condition, both PSD and % area of particulate were significantly lower in the outer circle (segments 5–8 and 13–16) ($0.034 +/- 0.017$, $0.020 +/- 0.010$) compared with the inner circle (segments 1–4 and 9–12) ($0.21 +/- 0.054$, $0.16 +/- 0.065$) ($p < 0.0001$, Mann–Whitney U test). There was a large amount of fluorescent debris attached to the undersurface of the OtoTent, which may account for the apparent reduced levels of particulate debris even in the inner circle compared with other test conditions (though this did not reach statistical significance as noted below) (Fig. 4C).

OtoTent Quantitatively Reduced Particle Dispersion Beyond the Boundaries of the Drape

Quantitative comparisons across simulation conditions were performed by grouping the segments of the octagonal grid into inner circles (segments 1–4 and 9–12) and outer circles (segments 5–8 and 13–16). Since the majority of the aerosolized particulates were found in quadrants A and B of the grid, an analysis of these two quadrants was performed to compare dispersion between the inner and outer areas across test conditions. In this analysis, particles found in the inner semicircle (segments 1–4) were compared with those of the outer semicircle (segments 5–8) closest to the surgeon. Particle dispersion in terms of PSD and %SA is shown in Figure 6A and B, respectively. In the inner semicircle, comparisons of PSD and %SA were not statistically significantly different across the three test conditions (Kruskall–Wallis test, $p = 0.074$ and $p = 0.39$, respectively). In the outer semicircle, comparisons of PSD and %SA were statistically significantly different across the three test conditions (Kruskall–Wallis test, $p = 0.0066$). There was a statistically significant difference in both PSD and %SA in the outer semicircle between drilling without a microscope and drilling with the microscope + OtoTent (two-stage linear step-up procedure for multiple comparisons, $p < 0.05$ for particle density and for percent surface area). Similarly, there was statistically significant difference in both PSD and %SA between drilling with a microscope and drilling with the microscope + OtoTent (two-stage linear step-up procedure for multiple comparisons, $p < 0.01$ for PSD and %SA).

Particulate Dispersion as a Function of Distance From the EAC

A subanalysis of segments 2 and 4 (see Fig. 2A for segment labeling), which had a high surface density of particulate matter, was performed by further subdividing the segments into trapezoidal segments with a 10 cm radius as measured from the center to the perimeter of the octagonal grid. The central 10 cm triangular segment was not counted because this area was covered by the cadaveric head specimen. For the no microscope and microscope conditions, both PSD (Fig. 6C) and %SA

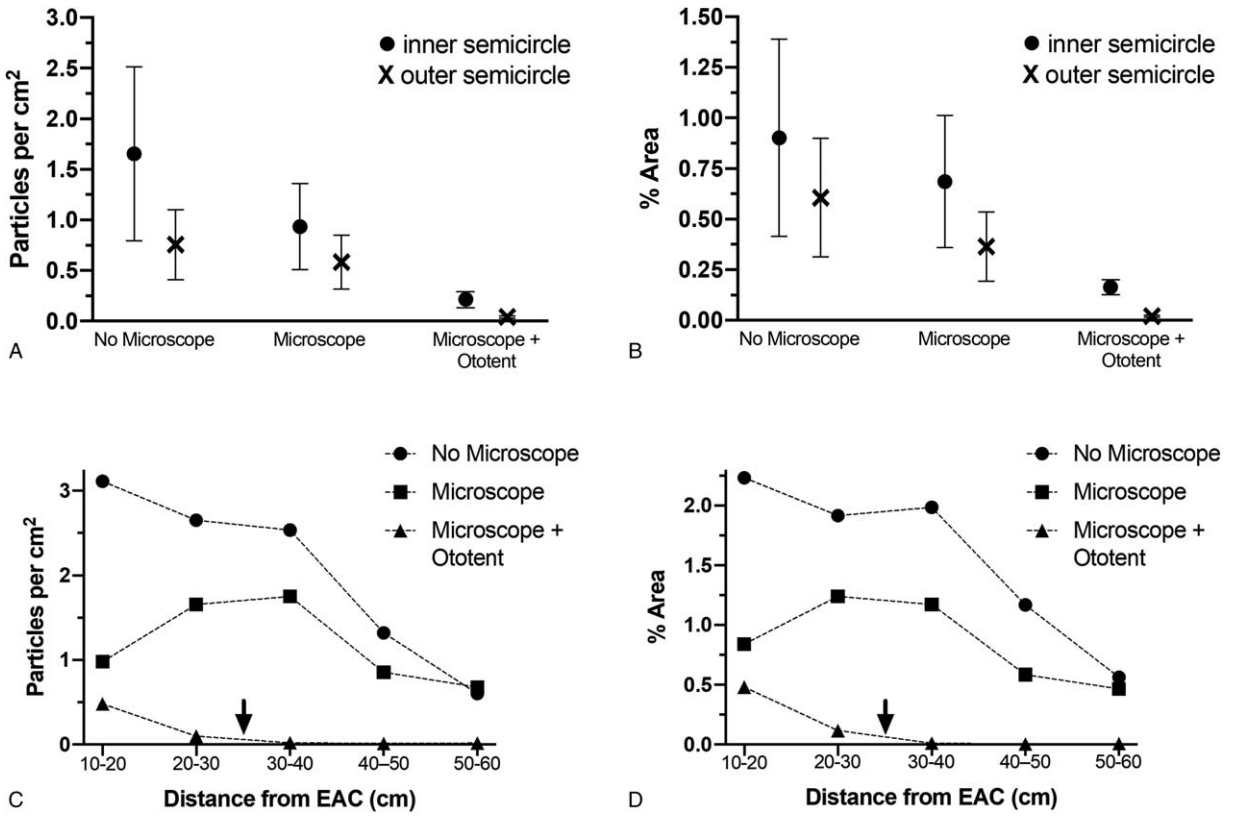

FIG. 6. Quantifying fluorescent particles under three test conditions: no microscope, microscope, and microscope + OtoTent. in terms of particle surface density (*A*) and percent (%) surface area covered by particles (*B*). The mean of the inner semicircle (segments 1–4) and outer semicircle (segments 5–8) is shown, with standard error bars. There was no significant difference in either particle surface density or % area covered when the inner semicircle segments were compared. The OtoTent condition showed significantly decreased particle surface density and % area covered when the outer semicircle was compared to the no microscope and microscope conditions. Particulate dispersion as a function of distance from the EAC (*C*, *D*) is shown based on a subanalysis of a single triangular wedge of the octagonal grid (segments 2 and 4). For both microscope and no microscope conditions, the particulate surface density and % area covered began to decrease beyond 40 cm from the EAC but were still present at 60 cm from the EAC. In the OtoTent condition, measured particulate density and % area approach zero beyond the OtoTent, which was fixed at a 30 cm radius. Down-pointing *arrow* denotes the location of the perimeter of the OtoTent at 30 cm away from the EAC.

(Fig. 6D) were highest between 10 and 40 cm and began to decrease at distances beyond 40 cm from the EAC. Note that there is still significant particulate measured at 60 cm from the EAC in both of these conditions. For the microscope + OtoTent condition, PSD and %SA were low inside the OtoTent and approached zero at distances greater than 40 cm from the EAC, representing the area outside the OtoTent.

High-flow and Low-flow Irrigation Conditions Did Not Significantly Change Particle Dispersion

Conditions with high- and low-flow irrigation did not significantly impact the patterns of aerosol and particulate dispersion (Supplemental Figure 1, http://links.lww.com/MAO/B25). In comparing nonmicroscope drilling conditions with different irrigation parameters (low-flow irrigation at 10 mL/min, high-flow irrigation at 20 mL/min, and no irrigation), PSD and %SA following drilling did not differ significantly between irrigation conditions for the inner semicircle (Kruskall–Wallis test, $p = 0.86$, $p = 0.71$, respectively) or outer semicircle of segments in the test grid (Kruskal–Wallis test, $p = 0.63$, $p = 0.65$, respectively).

DISCUSSION

Otolaryngologists are uniquely susceptible to COVID-19 transmission due to the variety of procedures performed on areas contiguous with the upper respiratory tract where there is a viral load (5,6). During this pandemic, otolaryngologists may be required to perform common surgeries for urgent indications and should prepare strategies to mitigate risk. These include preoperative COVID-19 testing (4), if timing and resources allow, as well as procedure-specific strategies to decrease the risk of transmission from patients who are at risk or positive for COVID-19. In this paper, we examined the risks of contamination with biomaterials during mastoidectomy and introduce a novel risk mitigation strategy using a modified operating room drape.

As a cortical mastoidectomy is the treatment for a number of serious complications of acute and chronic otitis media, this article aimed to characterize the spread of aerosolized materials during surgery that could potentially transmit virus. The precise definition of an aerosol is elusive in the medical literature, representing a range of particle sizes from those less than 5 μm in diameter that remain in the air for long durations leading to airborne spread, to larger aerosols that travel in the air less than 1 m leading to droplet transmission (15). Mycobacterium tuberculosis is a well-known airborne pathogen. SARS-CoV-2 is more likely to be a pathogen which typically transmits through larger aerosols but can become temporarily airborne during an aerosol-generating procedure (15). The use of high-powered drills has previously been demonstrated to generate a range of aerosol-sized particles (11,16). In this study, we demonstrated that mastoidectomy is an aerosol-generating procedure and quantitatively demonstrated the spread of small droplets more than 100 cm from the surgical site, with a predominance of spread in the areas closest to the operative site. Plumes of even smaller particles were easily visualized during mastoid drilling simulations but not able to be directly quantified. The experimental setup was designed in a 360-degree fashion to assess risk of aerosolized debris dispersion toward all operating room staff in close proximity, including the anesthesiologist and the scrub nurse or technician. While the majority of the particulate debris was found in the two quadrants adjacent to the surgeon, this study also demonstrates that cortical mastoidectomy may cause particulate spread in the two quadrants located opposite the surgeon. This highlights the importance of barrier drapes hung between the surgical site and the anesthesiologist. Furthermore, in this study, the right-handed surgeon spread aerosolized debris predominantly in the left lower quadrant of the field, followed by the right lower quadrant. This may have been impacted by accumulation of some particulate on the surgeon's arms and gown, reducing the measured particulate in the lower right quadrant. Aerosolized particles can be found all over the surgeon including on the gown, face shield, and hair covering. These findings corroborate previous studies examining the possibility of transmission of blood-borne and prion diseases during mastoidectomy, finding that drilling scatters blood-containing and neural tissue-containing material that could be detected on the surgical field and on the surgeon (12,13).

Although it is not known for certain whether aerosols of different sizes generated during mastoidectomy are capable of transmitting COVID-19, existing virology literature suggests that fluid in the inner ear and mastoid can be infected with respiratory viruses. Pitkaranta et al. demonstrated that viral RNA could be identified in 48% of middle ear fluid samples collected from children with an upper respiratory illness and acute otitis media when assessing for human coronavirus, respiratory syncytial virus, and human rhinovirus (14). Similarly, Heikkinen et al. (17) found that viral materials could be identified with enzyme immunoassays in 74% of middle ear fluid samples in children with acute otitis media when assessing for parainfluenza, influenza, respiratory syncytial virus, enterovirus, and adenovirus.

As yet, there are no formal guidelines on the best practices to reduce viral transmission during common otology or neurotology procedures, but novel techniques have recently been reported to mitigate the risk associated with oral intubation (18), extubation (19), and endoscopic sinus surgery (11). These strategies make use of various plastic materials to create physical barriers between the patient and the health care provider. In this study, as the microscope alone was shown to be an insufficient barrier, we piloted the use of a simple barrier drape, the OtoTent, to limit the spread of aerosols and droplets during mastoidectomy. The drape was easy to create and affix to the microscope. The authors found that fixing the tent posteriorly with tape between the surgeon's arms was critical to keeping the OtoTent in place during surgery. The surgeon's arms and instrument cords were easily passed between points of fixation with good range of motion. The OtoTent significantly reduced droplet and particulate contamination of surfaces beyond its borders within the limits of this study design. In addition, particulate debris inside the borders of the OtoTent on the surfaces of the cadaver's head and immediate surrounding area was also significantly reduced. This is likely due to particulate debris adhering to the undersurface of the OtoTent.

The OtoTent was created from a commercially available surgical drape commonly used for ophthalmologic procedures. Hospitals with ophthalmology divisions may already carry the 1,060 drape. The cost of the product is low, around $10 US. After applying a standard sterile drape to the microscope, the OtoTent may be attached to the microscope lens before otologic surgery or high-speed drilling commences. A microscope drape could be used as an alternative material, but may be more expensive, add bulk over the surgeon's lap, and may require more manipulation to affix it securely to the microscope. One advantage of using a microscope drape is that a second drape will almost certainly be available in the operating room. A setup similar to an OtoTent using a second microscope drape was separately conceived and elegantly illustrated by colleagues in the United Kingdom (personal communication) (20).

Various improvements can be made to the simple OtoTent design presented in this study. Further modifications will likely require real operating room experience and feedback. Surgeons who tried a modified OtoTent in the operating room at our institution (DHJ, DAC) reported it was relatively easy to use and seemed to reduce particulate dispersion (Fig. 7). However, particulate dispersion was not quantitatively assessed in the operating room. For the experimental study, the authors elected to tape four cardinal points on the drape to minimize movements to the drape with the surgeon's hand movements, whereas intraoperatively, surgeons

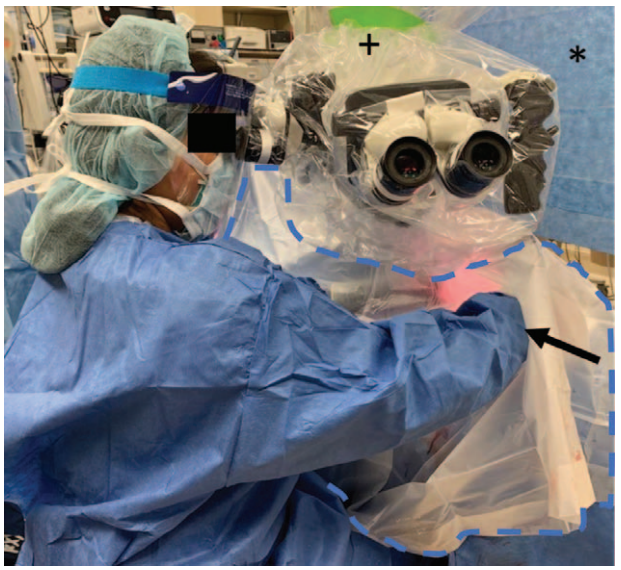

FIG. 7. Modified OtoTent (dotted blue outline) use in the operating room for a lateral skull base surgery. The setup shown here is similar, but not identical, to the experimental setup for the OtoTent. After a standard sterile microscope drape (+) was placed, a 9 cm diameter circle was cut out of the incise area of the 1,060 drape and the drape was attached to the lens mount of the Leica M525 OH4 microscope. The drape was then secured to the table with staples, and one portion of it was tucked into an otologic irrigation collection bag. Two small slits (one indicated with black *arrow*) were cut to accommodate the surgeon's arms. The otologic drill and suction irrigator passed underneath the drape. An additional barrier sheet (*) was hung to partition the surgical field from anesthesiologist.

may find that stapling the perimeter of the drape and incising the OtoTent to allow for the surgeon's arms may prove more ergonomic. Larger holes may need to be cut in the 1,060 drape to accommodate larger operating microscopes. Note that these possible variations were not quantitatively evaluated in this study. While drilling, the surgeon may find that the microscope lens needs to be cleaned as debris and moisture circulates under the OtoTent, so a wipe should be kept within easy reach. A surgical scrub technician could pass additional instruments underneath the other flaps of the OtoTent not occupied by the surgeon's two arms. At the conclusion of drilling, the OtoTent should be removed carefully so as not to dislodge and reaerosolize particles. It may be beneficial to wait a short time to allow for settling of at least the larger aerosolized particles. A second set of surgical gloves and arm sleeves could be used under the OtoTent and removed at the conclusion of drilling to minimize dispersion of particles landing on the surgeon. Because the OtoTent is not impervious around its perimeter, it is not a substitute for appropriate PPE and should only be used as an adjunct.

Even with success of a simple material barrier like the OtoTent, mastoidectomy may also produce microscopic aerosols that could remain airborne for an extended period of time. In this study, the visualization of plumes of fluorescent debris during mastoidectomy demonstrates that it is certainly an aerosol-generating procedure despite the limitations of this study to analyze particles smaller than 100 μm. Norris et al. conducted a cadaveric temporal bone study to sample aerosolized bone dust in the air during mastoidectomy and found that the average total particulate matter concentration was 1.89 mg/m (3,21). Although the authors concluded that this was below the Occupational Health and Safety Administration's standards for respirator use, they did not explore the idea that a small amount of particulate matter might be enough to transmit a virus.

What is yet unknown is the ability of the aerosolized materials produced during mastoidectomy (e.g., blood, bone dust, middle ear and mastoid mucosa and fluid) to transmit COVID-19 and whether the quantity and size of particles affects the transmission rate. As such, this study reinforces the recommendations in the existing literature to remain vigilant in the selection of appropriate PPE. At a minimum, for mastoidectomy surgery, basic OR attire with impervious gowns, gloves, hair coverings, and shoe coverings should be supplemented with face shields, ventless, or wrap-around eye protection and respirators. N95 respirators should be used as for all aerosol-generating procedures as recommended by multiple medical professional societies (22) and the World Health Organization (23). As mastoidectomy is an aerosol-generating procedure, we think that N95 masks are warranted when operating on COVID-19-positive patients, and even for patients with unknown COVID-19 status in areas with sustained community spread in the absence of a widely available, rapid turnaround test with high sensitivity (24). By definition, N95 masks block at least 95% of aerosols 0.3 μm in size (25), and are therefore capable of protecting surgeons from the particles sizes measured in this study. Powered air-purifying respirators (PAPRs) have been recommended in the field of orthopedic surgery and shown to decrease the biomaterials that touch the surgeon during bone drilling procedures (16). Given that a high degree of spread of aerosolized debris was found in this study and that particulate debris was found even in the hair covering after 1 minute of drilling, otologists could consider the use of a PAPR in addition to an N95 mask as this combination has been shown to have a multiplicative effect on reducing the concentration of airborne particles (26). However, with limited availability of PAPRs at most institutions, we recognize that obtaining PAPRs may not be possible. The use of PAPRs with microscope oculars may also be cumbersome, although it was possible to use a face shield with the microscope in this study. Exoscopes may be an alternative option in institutions with access to this technology.

The limitations of this study stem from constraints on the materials available to conduct these time-sensitive experiments during a time of medical crisis. The bone of cadaveric models may differ from those of living patients

in their biochemical properties, their reactions to drilling, and lack of mucous—all of which may impact dispersion. Future cadaveric studies could assess for dispersion of mucosal epithelial cells within the droplets. If studies could be repeated on patients with COVID-19, it would be possible to test dispersed droplets for virus. The authors also did not have access to equipment to measure the smallest aerosols that remain suspended in the air; the smallest particle that could be detected using techniques described in this article was 100 μm. Bone dust, which had significant autofluorescence, was unable to be distinguished from droplets containing fluorescein, although bone dust itself could be mixed with mastoid fluids during drilling and could also harbor viral particles. Furthermore, it was not possible to assess individual particles that may have conglomerated upon hitting experimental surfaces. Irrigation applied in the study could have diluted the concentration of fluorescein dye, although this was not shown to have a significant effect on particle distribution for the limited number of irrigations rates studied. Finally, alternate configurations of the operation were not tested including the use of different drill speeds, burr types (e.g., cutting versus diamond), burr sizes, suction irrigator sizes, other microscope sizes/configurations, other drilling techniques (including a left-handed surgeon), and the use of unconventional alternatives to high-speed drills such as osteotomes or hand-operated perforators. Limiting testing conditions was necessary to conserve resources including PPE. Lastly, the OtoTent was designed to be simple to allow for easy reproduction. More elaborate designs including the incorporation of gloves into the drape to minimize the escape of even smaller aerosolized materials or a vacuum system to further collect and sequester droplets and aerosols could also be considered. Further studies to address these deficiencies will be important as the COVID-19 pandemic evolves and strategies to resume less urgent surgical cases are developed.

CONCLUSION

Mastoidectomy is a high-risk aerosol generating procedure with the potential to expose the surgeon and operating room staff to infectious particles. Strategies including sufficient PPE with head, face and neck covering and the novel use of drapes should be explored to limit the spread of infectious materials generated by high-speed drilling.

Acknowledgments: The authors thank Andria LeDoux, RN, for assistance in arranging equipment for the Cadaver Laboratory.

REFERENCES

1. WHO Director-General's opening remarks at the media briefing on COVID-19—11 March 2020. Available at: https://www.who.int/dg/speeches/detail/who-director-general-s-opening-remarks-at-the-media-briefing-on-covid-19–11-march-2020. Accessed April 12, 2020.
2. Ranney ML, Griffeth V, Jha AK. Critical supply shortages — The need for ventilators and personal protective equipment during the Covid-19 pandemic. *N Engl J Med* 2020;382:e41.
3. Xu K, Lai X, Zheng L. Suggestions on the prevention of COVID-19 for health care workers in department of otorhinolaryngology head and neck surgery. *World J Otorhinolaryngol Head Neck Surg* 2020. [Epub ahead of print].
4. Patel Z, Fernandez-MIranda J, Hwang P, et al. Precautions for endoscopic transnasal skull base surgery during the COVID-19 pandemic. March 2020. Available at: https://med.uth.edu/orl/wp-content/uploads/sites/68/2020/03/Update-on-Precautions-Regarding-Endoscopic-Procedures-and-COVID-19-2020-03-22.pdf. Accessed April 10, 2020.
5. Vukkadala N, Qian ZJ, Holsinger FC, Patel ZM, Rosenthal E. COVID-19 and the otolaryngologist – preliminary evidence-based review. *Laryngoscope*. 2020 [Epub ahead of print].
6. Givi B, Schiff BA, Chinn SB, et al. Safety recommendations for evaluation and surgery of the head and neck during the COVID-19 pandemic. *JAMA Otolaryngol Head Neck Surg* 2020. [Epub ahead of print].
7. Brewster DJ, Chrimes NC, Do TB, et al. Consensus statement: Safe Airway Society principles of airway management and tracheal intubation specific to the COVID-19 adult patient group. *Med J Aust* 2020;[Epub ahead of print].
8. Meng L, Qiu H, Wan L, et al. Intubation and ventilation amid the COVID-19 Outbreak Wuhan's experience. *Anesthesiology* 2020. [Epub ahead of print].
9. Parker N, Schiff B, Fritz M, et al. Tracheotomy recommendations during the COVID-19 pandemic. March 2020. Available at: https://www.entnet.org/content/tracheotomy-recommendations-during-covid-19-pandemic. Accessed April 9, 2020.
10. Edwards SP, Kasten S, Nelson C, Elner V, McKean E. Maxillofacial trauma management during COVID-19: Multidisciplinary recommendations. *Facial Plast Surg Aesthet Med* 2020. [Epub ahead of print].
11. Workman AD, Welling DB, Carter BS, et al. Endonasal instrumentation and aerosolization risk in the era of COVID-19: Simulation, literature review, and proposed mitigation strategies. *Int Forum Allergy Rhinol* 2020. [Epub ahead of print].
12. Scott A, De R, Sadek SA, Garrido MC, Courteney-Harris RG. Temporal bone dissection: A possible route for prion transmission? *J Laryngol Otol* 2001;115:374–5.
13. Hilal A, Walshe P, Gendy S, Knowles S, Burns H. Mastoidectomy and trans-corneal viral transmission. *Laryngoscope* 2005;115:1873–6.
14. Pitkäranta A, Virolainen A, Jero J, Arruda E, Hayden FG. Detection of rhinovirus, respiratory syncytial virus, and coronavirus infections in acute otitis media by reverse transcriptase polymerase chain reaction. *Pediatrics* 1998;102:291–5.
15. Jones R, Brosseau L. Aerosol transmission of infectious disease. *J Occup Environ Med* 2015;57:501–8.
16. Makovicka JL, Bingham JS, Patel KA, Young SW, Beauchamp CP, Spangehl MJ. Surgeon personal protection: An underappreciated benefit of positive-pressure exhaust suits. *Clin Orthop Relat Res* 2018;476:1341–8.
17. Heikkinen T, Thint M, Chonmaitree T. Prevalence of various respiratory viruses in the middle ear during acute otitis media. *N Engl J Med* 1999;340:260–4.
18. Canelli R, Connor CW, Gonzalez M, Nozari A, Ortega R. Barrier enclosure during endotracheal intubation. *N Engl J Med* 2020. [Epub ahead of print].
19. Matava CT, Yu J, Denning S. Clear plastic drapes may be effective at limiting aerosolization and droplet spray during extubation: Implications for COVID-19. *Can J Anaesth* 2020. [Epub ahead of print].
20. Heller W, Mitchell T, Thomas S. Mastoidectomy in the COVID era—the 2 microscope drape method to reduce aerosolization. Available at: https://www.entuk.org/sites/default/files/Mastoidectomy%20in%20the%20COVID%20Era%20%E2%80%93%20-The%202.pdf. Accessed April 20, 2020.

21. Norris BK, Goodier AP, Eby TL. Assessment of air quality during mastoidectomy. *Otolaryngol Head Neck Surg* 2011;144: 408–11.
22. AANA, ASA, APSF and AAAA Issue Joint Statement on Use of Personal Protective Equipment During COVID-19 Pandemic. March 2020. Available at: https://www.aana.com/home/aana-updates/2020/03/20/aana-asa-and-apsf-issue-joint-statement-on-use-of-personal-protective-equipment-during-covid-19-pandemic. Accessed April 10, 2020.
23. Rational use of personal protective equipment for coronavirus disease (COVID-19) and considerations during severe shortages. April 2020. Available at: https://www.who.int/publications-detail/rational-use-of-personal-protective-equipment-for-coronavirus-disease-(covid-19)-and-considerations-during-severe-shortages. Accessed April 10, 2020.
24. Nalla AK, Casto AM, Huang M-LW, et al. Comparative performance of SARS-CoV-2 detection assays using seven different primer/probe sets and one assay kit. *J Clin Microbiol* 2020. [Epub ahead of print].
25. Health C for D and R. N95 Respirators and Surgical Masks (Face Masks). *FDA*. April 2020. Available at: https://www.fda.gov/medical-devices/personal-protective-equipment-infection-control/n95-respirators-and-surgical-masks-face-masks. Accessed April 22, 2020.
26. Roberge MR, Vojtko MR, Roberge RJ, Vojtko RJ, Landsittel DP. Wearing an N95 respirator concurrently with a powered air-purifying respirator: Effect on protection factor. *Respir Care* 2008;53: 1685–90.